Evaluation of new ceramic electrodes based on Sb-doped SnO_2 for the removal of emerging compounds present in wastewater

Julia Mora-Gómez[a], Montserrat García-Gabaldón[a*], Emma Ortega[a], María-José Sánchez-Rivera[b], Sergio Mestre[b,c], Valentín Pérez-Herranz[a]

[a]*IEC Group, Departament d'Enginyeria Quimica i Nuclear, Universitat Politècnica de València, Camí de Vera s/n, 46022, València, P.O. Box 22012, E-46071, Spain*

**Corresponding autor: Fax: +34-96-3867639; Tel:+34-96-3877632;*

E-mail: mongarga@iqn.upv.es

[b]*Instituto Universitario de Tecnología Cerámica, Universitat Jaume I, Castellón, Spain.*

[c]*Departamento de Ingeniería Química. Universitat Jaume I, Castellón, Spain.*

Abstract

The properties of the ceramic electrodes make them interesting for electrochemical advanced oxidation processes (EAOPs), destined to the elimination of emergent or refractory contaminants, as an alternative to boron-doped-diamond (BDD) electrodes. For this purpose, new ceramic electrodes based on Sb-doped SnO_2 have been developed. Sb-doped tin oxide electrodes have been obtained through mechanical mixing of raw materials and sintering of dry-pressed specimens. Different sintering temperatures (1050 °C to 1250 °C) were considered. The electrochemical behavior of the resulting electrodes has been compared to that exhibited by Pt and BDDs electrodes. The oxygen discharge potential (E_{O2}) for the ceramic electrodes decreases as the sintering temperature increases, being these values higher than that observed for the Pt electrode and smaller than that for the BDD electrode. This result in a highest rate of

COD removal for the electrode sintered at 1050 ºC comparing with the rest of ceramic electrodes under potentiostatic operation. On the other hand, in galvanostatic mode, the performance of the different ceramic electrodes in terms of the degradation of Norfloxacin, used as tested antibiotic, was similar.

Comparing the behavior of the ceramic electrode sintered at 1250 ºC and that of the BDD electrode at an applied potential of 3V, it is inferred that although both present similar values in terms of the degradation of Norfloxacin, the rate of removal of the chemical oxygen demand is higher in the case of the BDD.

Keywords: BDD, ceramic electrode, electrochemical advanced oxidation processes, Norfloxacin.

1. Introduction

Developed countries have overcome industrialization processes. These processes have a number of advantages, such as improving the living conditions of the residents of these countries. However, also involve negative aspects, as the release of pollutants into wastewater [1,2]. As a result of this problem, legislation is getting increasingly more restrictive. Usually, the treatment of waste water is carried out with physico-chemical and biological methods. Physico-chemical methods are based on the separation of pollutants from the water stream using processes such as precipitation, decantation or flotation of the compounds, by the possible addition of chemical agents. Biological methods are very useful to biodegradable compounds, since they are effective and their cost is low. However, this conventional technique does not completely eliminate all

types of contaminants, such as refractory organic compounds and emerging compounds [3]. Therefore, it is necessary to develop new techniques capable of degrading these compounds.

In recent years, electrochemical advanced oxidation processes (EAOPs) are focused on the removal of these compounds in wastewater, due to their versatility, high energy efficiency and the absence of chemical additives [4,5]. These technologies are based on the electrochemical generation of strong oxidants, such as hydroxyl radicals (OH•). The most important component in EAOPs is the electrode with anodic function. This electrode should be stable, cheap, easy to synthesize and must have a high electrochemical activity. Anodes can be classified into two types: "active" and "non-active" anodes. In the "active" anodes (such as graphite, Pt or oxides of noble metals) hydroxyl radicals are sorbed on the surface of the anode and oxidized to oxygen atoms, which are covalently bound to the anode, so oxidation is limited to the surface of the electrode. These anodes are not the most suitable for mineralizing complex substances [6]. In contrast, at the "inactive" anodes the hydroxyl radicals are sorbed at the surface of the anode, but these electrodes are not covalently bound to oxygen atoms. These radicals are very reactive and they act indiscriminately [4]. Examples of "inactive" anodes are boron-doped diamond (BDD) and oxides of Sn and Pb [7].

Nowadays, the most widely used electrodes on a laboratory and pilot-scale are the BDDs [5,8]. These electrodes have a number of advantages compared to others: (i) high oxygen overpotential, whereby the hydroxyl radicals generated have in-depth oxidizing power [9]; (ii) their stability as anode, which is due to sp^3 hybridization of C atoms [10]; and (iii) a wide working potential window [11]. This substrate must exhibits low

electrochemical activity, high conductivity, low cost and low fragility [5,10]. An alternative to boron-doped diamond electrodes are the ceramic electrodes. These promising electrodes present a low price, a high active area [12] due to its porosity; a high chemical stability and their manufacture is relatively easy. The most studied ceramic electrode is the Ebonex®, whose composition is predominantly Ti_4O_7 (a non-stoichiometric oxide of titanium). This electrode shows good conductivity (more than graphitic carbon) and a high oxygen evolution potential [12]. Its main drawback is the change in its surface composition towards stoichiometric oxides when it is subjected to anodic polarization, which present worse properties as anode [13].

For this purpose, in this work, new manufactured ceramic electrodes based on tin oxide will be studied. Tin oxide exhibits many attractive physical and chemical properties, such as high conductivity (n-type semiconductor) and corrosion resistance. In pottery and tile manufacture, SnO_2 has been used as opacifier in glazes [14] and as raw material for the chrome-tin pink and some other pigments [15]. Along the last decades, it has been increasingly used in components requiring high chemical corrosion resistance in chemical industry applications [16,17]. In the last field, an important application is obtaining electrodes for electric glass melting furnaces [18,19] and the processing of aluminium by electrolysis [17,20,21]. Stoichiometric tin oxide is a good insulator at room temperature. However, natural and synthetic oxides have oxygen deficiencies leading to the semiconductivity. In addition, the electrical conductivity could be increased by doping with some oxides. Sb_2O_3 is the most extended one in industrial applications [21]. One of the main difficulties in obtaining SnO_2 electrodes is its poor sinter ability that hinders its use [22–25]. Different approaches have been used to improve densification. The traditional solution was the addition of other metallic oxides

as “sintering aids” [26–28]. In this case the usual mechanism is the formation of a eutectic liquid between SnO_2 and the “sintering aid” at low temperature which favors a liquid-phase sintering. However, more sophisticated sintering techniques has been applied to SnO_2 sintering, as hot isostatic pressing [29,30], field activated sintering technique (FAST) [31,32] or electric field-assisted sintering [33].

The objective of this paper is the electrochemical study of these new ceramic electrodes that must be capable of competing with the BDD electrodes, to be used as anodes in the oxidation of refractory and emerging compounds. Their electrochemical characterization will be carried out by means of two processes: the polarization curves and the treatment of an emerging compound. The selected emerging compound to be degraded is an antibiotic, the 1-ethyl-6-fluoro-4-oxo-7-piperazin-1-yl-1H-quinoline-3-carboxylic acid, commonly referred as Norfloxacin (NOR), due to its persistence in conventional water treatment plants [1,34]. In addition, the evolution of chemical oxygen demand (COD), which is another determining factor for the discharge into the environment, will be monitored. The results obtained are compared with those obtained with a BDD electrode.

2. Materials and methods

2.1 Synthesis of the electrodes

Electrode’s raw material were SnO_2 (purity 99.85 %, Quimialmel S.A., Spain), and Sb_2O_3 as dopant (purity 99 %, Alfa-Aesar, Germany). A composition with a molar relation SnO_2/Sb_2O_3 equal to 98/2 was formulated. 0.8% in weight of polivinylalcohol (Mowiol 8-88, Clariant Iberica S.A. Spain), was added to the composition as a ligand.

The raw materials were mixed in alumina jars with a planetary mill (Pulverisette 5, Fritsch GmbH, Germany), at 230 rpm during an hour using water as a fluid. The obtained suspension was dried in an oven at 110 °C for 24 h. The dry powder was sieved trough a 600 μm mesh and moistened to 5.2 % (kg water/kg dry solid). Prismatic specimens of 40x5x5 mm were obtained by dry pressing with a specific mold in a laboratory uniaxial manual press (Robima S.A., Spain), working at 250 $kg \cdot cm^{-2}$. Finally, the samples were sintered in a laboratory furnace (RHF1600, Carbolite Furnaces, UK). Five different maximum temperatures were employed between 1050 ºC and 1250 ºC, with a common temperature profile (heating at 15 $ºC \cdot min^{-1}$ from room temperature to maximum temperature, four hours at maximum temperature and cooling). At least three samples were sintered in each cycle.

2.2 Physical and morphological analysis of the electrodes

Bulk density of green specimens was measured by mercury immersion (Archimedes' method). The electrical resistivity of sintered samples was measured by a four points method with a Fluke 743B equipment (Fluke Corporation, USA), with a homemade setup. Then, bulk density of sintered samples was also measured by mercury immersion. The data allowed the calculation of weight loss, relative density and volumetric contraction after the thermal cycle.

The pore size distribution of sintered samples was obtained by mercury intrusion (AutoPore IV 9500, Micromeritics, USA). In addition, SEM images were taken with a FEG-SEM (QUANTA 200F, FEI Co, USA) from polished sections of sintered specimens. Characterization of crystalline structures present on some specimens was performed using an X-ray diffractometer (Theta-Theta D8 Advance, Bruker, Germany),

with CuK radiation (λ = 1.54183 Å). The generator applied an intensity light source of 45 kV and 40 mA. XRD data were collected by means of a VÅNTEC-1 detector in a 2θ from 5 to 90º with a step width of 0.015º and a counting time of 1.2 s/step.

2.3 Electrochemical characterization of the electrodes

The electrochemical studies were carried out with a potentiostat/galvanostat (Autolab PGSTAT302N) with a conventional three-electrode cell (Fig. 1). Three types of electrodes were tested as working electrodes: a ceramic electrode of SnO_2 doped with antimony; a BDD electrode and a Pt electrode. As counter and reference electrodes a Pt, and an Ag/AgCl, encapsulated with 3 M KCl, electrodes were used, respectively. All the experiments were performed at room temperature.

Before each electrochemical study, the ceramic and BDD electrodes, were subjected to an anodic polarization with 0.5M H_2SO_4 (J.T. Baker®) at 50 $mA \cdot cm^2$ to activate their surfaces and remove residual substances from the electrode surface [35,36].

2.3.1. Polarization curves

The anodic polarization curves were carried out from the OCP (open circuit potential) until reaching 3 V. The scan rate was 10 $mV \cdot s^{-1}$. A 50 ml of 2g/l Na_2SO_4 (Panreac®) under static conditions, was considered in these assays, in which the oxygen discharge potential (E_{O2}) was obtained. This parameter was found at the intersection of the linear extrapolation of the curve zone in the more anodic potentials (between 2 and 3 V) with the X axis.

2.3.2. Electrochemical treatment of NOR

Electrochemical experiments were performed in a 110 ml solution of 100 ppm of NOR (Sigma-Aldrich) and 2 g/l Na_2SO_4 as supporting electrolyte, at room temperature and under stirring during 5 hours. Two working modes were carried out: galvanostatic mode (constant applied current) and potentiostatic mode (constant electrode potential). The ceramic working electrodes used in these experiments were the same as those used in the polarization curves, and possess a geometric area of 7.5 cm^2. The BDD electrode employed had a doping level of 10000 ppm and the same geometric area as those of the ceramic electrodes.

Samples were taken from the electrochemical cell every 30 min, and potential, current, cell voltage and pH were recorded during electrolysis. For each sample, the evolution of NOR concentration was monitored using an Unicam UV4-200 UV/VIS Spectrometer at 315 nm. The COD measurement was based on the reaction of the sample with a strong oxidant, namely potassium dichromate (Panreac®), in which the Cr (VI) was reduced to Cr (III) as a function of the amount of organic matter present in the samples.

3. Results and discussion

3.1 Electrodes characterization

The colour of the sintered specimens was bluish-grey, more saturated as the maximum temperature increased. This behaviour pointed to a progressive formation of the blue Sb_2O_3-SnO_2 solid solution [37]. However, the weight loss showed a sharp increase between 1100 °C and 1200 °C (Fig. 2), suggesting that some transition is superimposed on Sb_2O_3 diffusion in SnO_2 network. Considering that the composition contained approximately a 0.8 wt% of PVA and the loss on ignition at 1300 °C of the used SnO_2 is

0.33 %, the obtained mass losses probably include a partial volatilization of antimony oxide, which begins around 500 °C [38], although its boiling point exceeds 1400 °C. Under this supposition, the fraction of initial antimony oxide volatilized was calculated (second axis of Fig. 2). The results showed that up to a 21 % of the Sb_2O_3 initially present could have been lost as the T_{max} of the sintering treatment increases. However, the remaining antimony oxide increases its diffusion into the SnO_2 network as the bluish-grey colour of the samples saturates. Probably the same mechanism which allows the loss of Sb_2O_3, also allows the depositions of this oxide in all the free surface of SnO_2 particles, favouring the formation of the solid solution.

The effect of Sb-doping was reflected in the resistivity of the samples (Fig. 3), which was low enough to allow the use of the specimens as electrodes. Concretely, the obtained values are of the same order of magnitude that those recommended for melting glass electrodes [21]. In addition, the resistivity shows a decrease in the same interval as the antimony losses increases, pointing to a better diffusion of antimony oxide in the tin oxide network as stated previously.

The sintered specimens showed a relative density nearly constant considering the uncertainty of the data (Fig. 4). However, there was detected a slight volumetric contraction in the sintered specimens, which increases with the maximum temperature, showing a trend similar to the one observed for weigh loss. In consequence, weight loss nearly compensates volumetric contraction during sintering, maintaining the relative density of sintered specimens in a narrow range. On the other hand, some sintering mechanism that facilitates the densification of the specimen starts at 1200 °C, that

superimposes to the gas phase transport mechanism that characterizes the sintering of SnO_2 at lower temperatures.

The small volumetric contraction of the samples was reflected on the pore size distribution curves, which showed a small but clear displacement of the pore size distribution towards higher diameters as sintering temperature increased (Fig. 5), together with a slight decrease in the total pore volume. In addition, the mean pore diameters (d_{16}, d_{50} and d_{84}) nearly tripled along the analysed temperature interval, showing a parabolic trend with the sintering temperature (Fig. 6). The SEM images show a progressive disappearance of the smaller particles and the growth of the larger particles, according to the Ostwald ripening phenomena (Fig. 7). In addition, the pores also grew to some extent, which is consistent with the results of the porosimetry. No trace of Sb_2O_3 particles was found, which was coherent with a gas-phase transport along the porous network. However, it must be considered that Sb and Sn are difficult to distinguish in the EDX analysis, as those elements are contiguous in the periodic table. In consequence, a low proportion of Sb_2O_3 over the surface or inside the particles of SnO_2 may be below the detection limit of the technique. On the other hand, the microstructure does not show critical changes with the sintering temperature. In consequence, the resistivity of the specimens would be governed by the doping level of SnO_2, and not by the microstructure.

3.2 Measurements of the oxygen discharge potential (E_{O2})

The values of the potential corresponding to the oxygen discharge of the different working electrodes tested are presented in Table 1. As can be observed, for the ceramic electrodes, E_{O2} decreases when the sintering temperature increases. This trend is related

to its resistivity (ρ), since it was previously verified that the resistivity decreases when the sintering temperature increases (Fig. 3). Therefore, the less conductive the electrode is, the greater E_{O2} presents. Comparing the values of the ceramic electrode with the Pt and BDD electrodes, it is noted that the potential values of the ceramic electrodes are higher than those corresponding to the Pt electrode and smaller than the BDD electrode. In order to degrade organic compounds in wastewater and to prevent the formation of "poisoned species" on the anode surface [39,40], it is interesting that the oxygen discharge potential is high (wide electrochemical window). Therefore, according to these results, the most suitable ceramic electrode is that sintered at the lowest temperature (1050 ºC).

3.3 Degradation of Norfloxacin

Fig. 8 shows the evolution of the concentration of NOR for the different ceramic electrodes at a constant applied current of 15 mA. Fixing the current value (15 mA) leads to impose the velocity of the oxidation reaction that take place. In the particular case presented in Figure 8, all the curves present the same shape (exponential decrease) due to the current regime, i.e., since in all the cases the current applied is higher than the limiting value corresponding to the norfloxacin oxidation. Moreover, the NOR degradation values present similar values, except for the experiment performed for the ceramic electrode sintered at 1250 ºC. A possible explanation of this difference could be attributed to the different microporous structure of the ceramic electrodes employed (Fig. 7). This fact makes that the electrochemically active surface of the electrodes differs from the geometric area, and therefore, although the applied current be the same in every case (15 mA), the effective current density could be different for each electrode.

The effect of the sintering temperature of the ceramic electrode (at 1050 and 1250 ºC) on the degradation of Norfloxacin and on the COD removal is presented in Fig. 9 (a) and (b), respectively, at an applied potential of 2.5 V. The more efficient electrode in degrading the NOR was that sintered at higher temperature, because as it presented lower resistance, the current reached is higher. With the electrode sintered at 1250 ºC an average current of 22.6 mA, corresponding to a NOR degradation of 73.5 % was obtained, whereas with the electrode sintered at the lowest temperature only 6 mA of current was reached, which led to a 56 % of the NOR degradation after 300 min. However, since the electrode sintered at 1050 ºC possesses the highest EO_2 (Table 1), the effect of the parasitic reactions are lower and this fact results in a highest rate of COD removal, which is an important aspect (Figure 9 (b)).

The effect of the electrode potential on the NOR degradation and on COD was also studied and is presented in Fig. 10 for two electrode potential values (2.5 and 3 V). In these cases, the average current values were 100 mA and 22.6 mA for 3 and 2.5 V, respectively. Hence, in the case of the highest electrode potential value it was possible to eliminate the 94 % of the initial concentration of NOR compared with the experiment performed at 2.5 V where the amount degraded was about 73.5 % (Fig. 10(a)). This remarkable increase in the percentage of degradation is due to the difference between the current values reached.

As observed in Fig. 10(b), the COD does not decrease in the same way as the NOR degradation. This may be due to the formation of new by-products of the emergent compound. The percentage of COD removal is about 50 % for an electrode potential of 3 V, whereas in the case of 2.5 V only a 33.8 % of COD was eliminated.

Finally, the behavior of the ceramic electrode sintered at 1250 °C and that of the BDD electrode is compared in Fig. 11 for an applied potential of 3 V. With the BDD electrode a degradation of 90% of the antibiotic and a removal of the COD of 60% was reached. In the case of the ceramic electrode a NOR degradation value of 94 % together with a 50 % of the COD removal was obtained. Therefore it can be concluded that for this potential value, the behavior of the BDD is better in terms of the elimination of the total organic matter, since although the electrode sintered at the highest temperature presents a behavior similar to that observed for the BDD electrode related to the NOR degradation, this substance could be oxidized to other toxic substances.

4. Conclusions

New ceramic electrodes have been designed using SnO_2 as raw material and Sb_2O_3 as dopant in alumina jars. The effect of different sintering temperatures of the ceramic electrodes has been investigated. An increase in the sintering temperature (between 1050-1250 °C) causes a greater volatilization of the antimony oxide. This volatilization produces an increase in the weight loss of the sample, and favors the deposition of Sb_2O_3 on the free surface of SnO_2 particles. Due to this increase in the deposition of Sb_2O_3 with the sintering temperature, the resistivity in the samples decreases. As the sintering temperature increases, a higher volumetric contraction of the electrodes is also observed. The relative density is kept constant for this range of sintering temperatures. This is due to the fact that the volume contraction is compensated by the loss of weight. The grain and pore size also increased with the sintering temperature.

The electrochemical characterization of the electrodes revealed that the oxygen discharge potential value decreases with the resistivity. Therefore, the electrode sintered at 1050 °C presents the highest oxygen discharge potential, and this fact is reflected by a highest rate of COD removal when comparing with the rest of ceramic electrodes under potentiostatic operation. At a constant applied current, all the curves present the same shape (exponential decrease) since in all the cases the current applied is higher than the limiting value corresponding to the norfloxacin oxidation, and the NOR degradation values present similar values.

Finally, comparing the behavior of the ceramic electrode sintered at 1250 ºC and that of the BDD electrode at an applied potential of 3V, it is inferred that although both present similar values in terms of the degradation of Norfloxacin, the removal rate of the chemical oxygen demand is higher in the case of the BDD.

Acknowledgments

The authors thanks to Ministerio de Economia y Competitividad and Fondo Europeo de Desarrollo Regional the support to this research [project number: CTQ2015-65202-C2-1-R and CTQ2015-65202-C2-2-R (MINECO/FEDER)].

References

[1] E. Gracia-Lor, J. V. Sancho, R. Serrano, F. Hernández, Occurrence and removal of pharmaceuticals in wastewater treatment plants at the Spanish Mediterranean

area of Valencia, Chemosphere. 87 (2012) 453–462.

[2] Y. Yavuz, R. Shahbazi, Anodic oxidation of Reactive Black 5 dye using boron doped diamond anodes in a bipolar trickle tower reactor, Sep. Purif. Technol. 85 (2012) 130–136.

[3] O. Ganzenko, D. Huguenot, E.D. Van Hullebusch, G. Esposito, M.A. Oturan, Electrochemical advanced oxidation and biological processes for wastewater treatment: a review of the combined approaches, Environ. Sci. Pollut. Resist. 21 (2014) 8493–8524.

[4] F.C. Moreira, R.A.R. Boaventura, E. Brillas, V.J.P. Vilar, Electrochemical advanced oxidation processes : A review on their application to synthetic and real wastewaters, Applied Catal. B, Environ. 202 (2017) 217–261.

[5] C. Comninellis, G. Chen, Electrochemistry for the Environment, Springer, New York, 2010.

[6] D. Bejan, E. Guinea, N.J. Bunce, On the nature of the hydroxyl radicals produced at boron-doped diamond and Ebonex® anodes, Electrochim. Acta. 69 (2012) 275–281.

[7] Q. Dai, J. Zhou, X. Meng, D. Feng, C. Wu, J. Chen, Electrochemical oxidation of cinnamic acid with Mo modified PbO_2 electrode: Electrode characterization, kinetics and degradation pathway, Chem. Eng. J. 289 (2016) 239–246.

[8] D.A.C. Coledam, J.M. Aquino, B.F. Silva, A.J. Silva, R.C. Rocha-Filho, Electrochemical mineralization of norfloxacin using distinct boron-doped diamond anodes in a filter-press reactor, with investigations of toxicity and oxidation by-products, Electrochim. Acta. 213 (2016) 856–864.

[9] A. Cruz-Rizo, S. Gutiérrez-Granados, R. Salazar, J.M. Peralta-Hernández, Application of electro-Fenton/BDD process for treating tannery wastewaters with

industrial dyes, Sep. Purif. Technol. 172 (2017) 296–302.

[10] B.P. Chaplin, Critical review of electrochemical advanced oxidation processes for water treatment applications, Environ. Sci. Process. Impacts. 16 (2014) 1182–1203.

[11] A. Kapałka, G. Fóti, C. Comninellis, The importance of electrode material in environmental electrochemistry Formation and reactivity of free hydroxyl radicals on boron-doped diamond electrodes, Electrochim. Acta. 54 (2009) 2018–2023.

[12] S. You, B. Liu, Y. Gao, Y. Wang, C.Y. Tang, Y. Huang, Monolithic Porous Magnéli-phase Ti_4O_7 for Electro-oxidation Treatment of Industrial Wastewater, Electrochim. Acta. 214 (2016) 326–335.

[13] D. Bejan, J.D. Malcolm, L. Morrison, N.J. Bunce, Mechanistic investigation of the conductive ceramic Ebonex® as an anode material, Electrochim. Acta. 54 (2009) 5548–5556.

[14] J. Molera, T. Pradell, N. Salvado, M. Vendrell-Saz, Evidence of Tin Oxide Recrystallization in Opacified Lead Glazes, J. Am. Ceram. Soc. 82 (1999) 2871–2875.

[15] G. Monrós, J.A. Badenes, A. García, M.Á. Tena, El Color de la Cerámica: nuevos mecanismos en pigmentos para los nuevos procesados de la industria cerámica, Publicaciones de la Universitat de Jaume I, Castelló de la Plana, 2013.

[16] S. Zuca, M. Terzi, M. Zaharescu, K. Matiasovsky, Contribution to the study of SnO_2-based ceramics. Part II: Effect of various oxide additives on the sintering capacity and electrical conductivity of SnO_2, J. Mater. Sci. 26 (1991) 1673–1676.

[17] L. Cassayre, T.A. Utigard, S. Bouvet, Visualizing Gas Evolution on Graphite and Oxygen-Evolving Anodes, JOM. 54 (2002) 41–45. doi:10.1007/BF02701696.

[18] C. Barry Carter, M. Grant Norton, Ceramic Materials Science and Engineering, Springer, New York, 2013.

[19] S. Yanagiya, N. V Nong, J. Xu, M. Sonne, N. Pryds, Thermoelectric Properties of SnO_2 Ceramics Doped with Sb and Zn, J. Electron. Mater. 40 (2011) 674–677.

[20] A. Popescu, S. Mihaiu, S. Zuca, Microstructure and Electrochemical Behaviour of some SnO_2 -based Inert Electrodes in Aluminium Electrolysis, Zeitschrift Für Naturforsch. A. 57 (2002) 71–75.

[21] A.J. Moulson, J.M. Herbert, Electroceramics: Materials, Properties, Applications, John Wiley & Sons, 2003.

[22] J. Fan, H. Zhao, Y. Xi, Y. Mu, F. Tang, R. Freer, Characterisation of SnO_2–CoO–MnO–Nb_2O_5 ceramics, J. Eur. Ceram. Soc. 30 (2010) 545–548.

[23] J. He, Z. Peng, Z. Fu, C. Wang, X. Fu, Effect of ZnO doping on microstructural and electrical properties of SnO_2–Ta_2O_5 based varistors, J. Alloys Compd. 528 (2012) 79–83.

[24] D. Nisiro, G. Fabbri, G.C. Celotti, A. Bellosi, Influence of the additives and processing conditions on the characteristics of dense SnO_2-based ceramics, J. Mater. Sci. 38 (2003) 2727–2742.

[25] Z.M. Jarzebsky, J.P. Marton, Physical Properties of SnO Materials. I Preparation and defect estructure, J. Electrochem. Soc. 123 (1976) 199–205.

[26] M.F. Bhopal, D. Lee, A. Rehman, S.H. Lee, Influence of annealing temperature on structural properties of ITO thin-films on graphite substrate, Vacuum. 133 (2016) 108–113.

[27] J.A. Cerri, E.R. Leite, D. Gouvêa, E. Longo, J.A. Varela, Effect of Cobalt(II) Oxide and Manganese(IV) Oxide on Sintering of Tin(IV) Oxide, J. Am. Ceram. Soc. 76 (1996) 799–804.

[28] C.R. Foschini, L. Perazolli, J.A. Varela, Sintering of tin oxide using zinc oxide as a densification aid, J. Mater. Sci. 39 (2004) 5825–5830.

[29] H. Kim, R.C.Y. Auyeung, A. Piqué, Transparent conducting F-doped SnO_2 thin films grown by pulsed laser deposition, Thin Solid Films. 516 (2008) 5052–5056.

[30] S.J. Park, K. Hirota, H. Yamamura, Densification of nonadditive SnO_2 by hot isostatic pressing, Ceram. Int. 10 (1984) 116.

[31] K.A. John, R.R. Philip, P. Sajan, T. Manju, In situ crystallization of highly conducting and transparent ITO thin films deposited by RF magnetron sputtering, Vaccum. 132 (2016) 91–94.

[32] O. Scarlat, S. Mihaiu, G. Aldica, J. Groza, M. Zaharescu, Semiconducting densified SnO_2-ceramics obtained by a novel sintering technique, J. Eur. Ceram. Soc. 24 (2004) 1049–1052.

[33] E.N.S. Muccillo, R. Muccillo, Electric field-assisted sintering of tin dioxide with manganese dioxide addition, J. Eur. Ceram. Soc. 34 (2014) 3699–3706.

[34] A. Özcan, A. Atılır Özcan, Y. Demirci, Evaluation of mineralization kinetics and pathway of norfloxacin removal from water by electro-Fenton treatment, Chem. Eng. J. 304 (2016) 518–526.

[35] A. Medel, E. Bustos, L.M. Apátiga, Y. Meas, Surface Activation of C-sp^3 in Boron-Doped Diamond Electrode, Electrocatalysis. 4 (2013) 189–195.

[36] E. Hmani, Y. Samet, R. Abdelhédi, Electrochemical degradation of auramine-O dye at boron-doped diamond and lead dioxide electrodes, Diam. Relat. Mater. 30 (2012) 1–8.

[37] M.I.B. Bernardi, S. Cava, E.R. Leite, C.A. Paskocimas, E. Longo, Comparison of blue pigments prepared by two different methods, J. Eur. Ceram. Soc. 22 (2002) 2911–2919.

[38] R.G. Orman, D. Holland, Thermal phase transitions in antimony (III) oxides, J. Solid State Chem. 180 (2007) 2587–2596.

[39] C. Comninellis, Electrocatalysis in the electrochemical conversion/combustion of organic pollutants for waste water treatment, Electrochim. Acta. 39 (1994) 1857–1862.

[40] R. Kötz, S. Stucki, B. Carcer, Electrochemical waste water treatment using high overvoltage anodes. Part I: Physical and electrochemical properties of SnO_2 anodes, J. Appl. Electrochem. 21 (1991) 14–20.

List of Figures

List of Tables

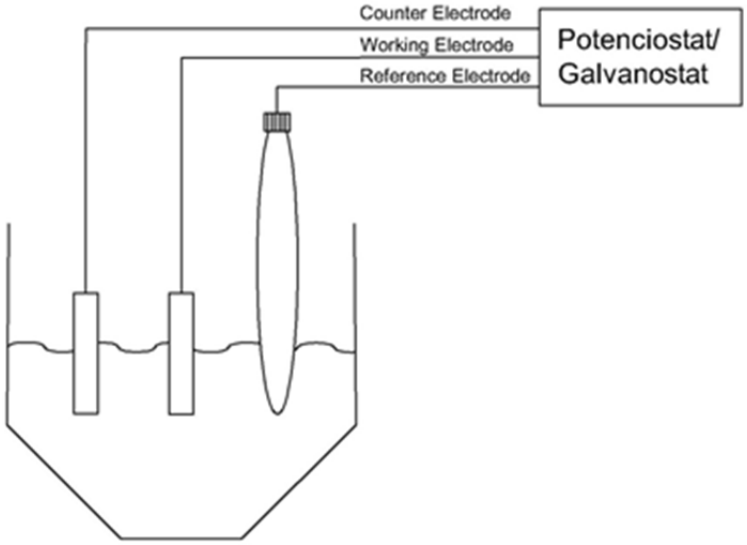

Figure 1. Scheme of experimental set up.

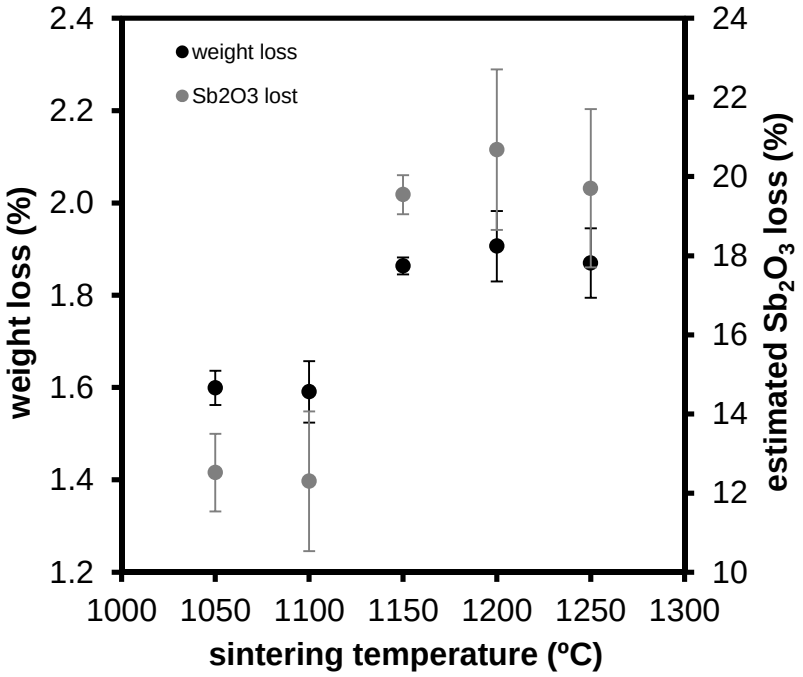

Figure 2. Evolution with sintering temperature of the weight loss of the specimens and the estimated antimony oxide loss.

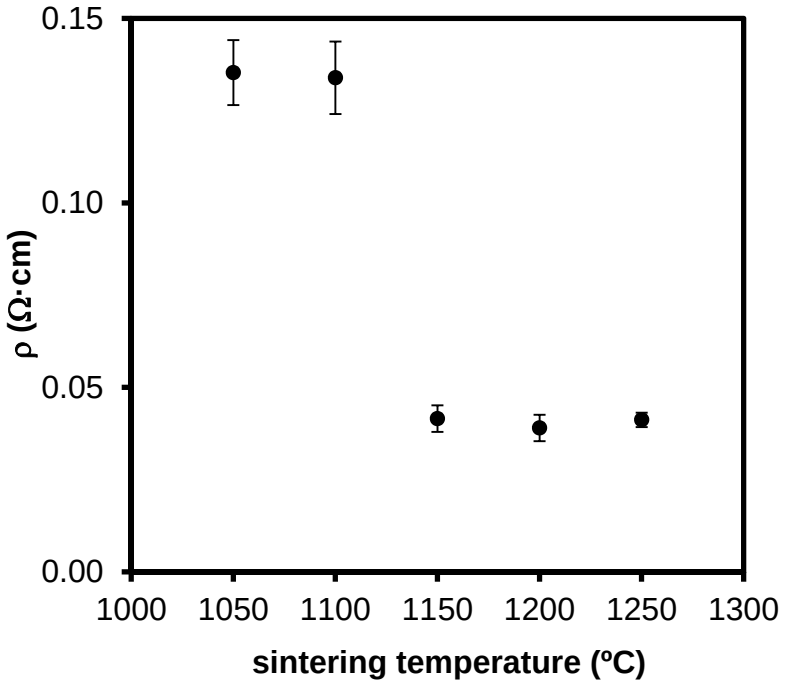

Figure 3. Evolution with sintering temperature of the resistivity of the specimens.

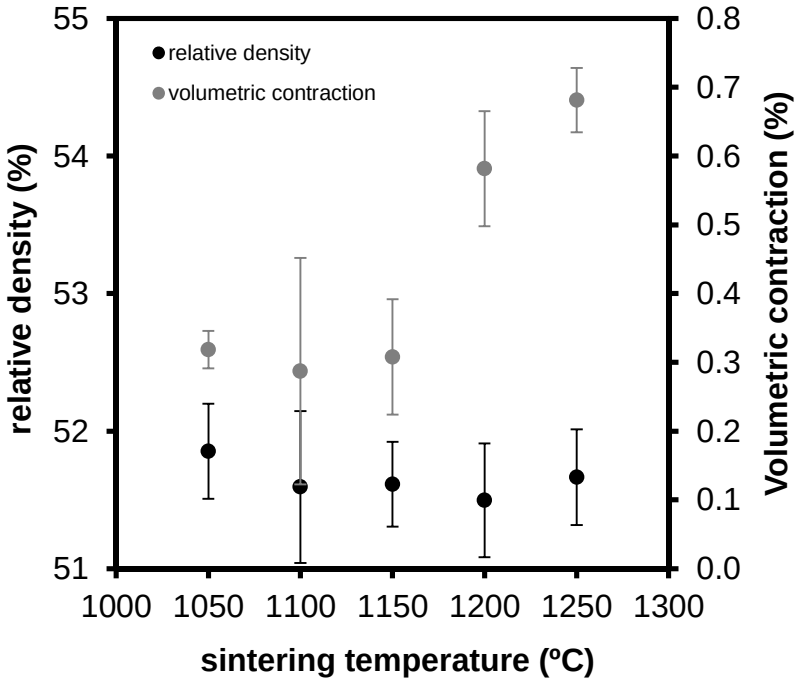

Figure 4. Evolution with sintering temperature of the relative density and the volumetric contraction of specimens.

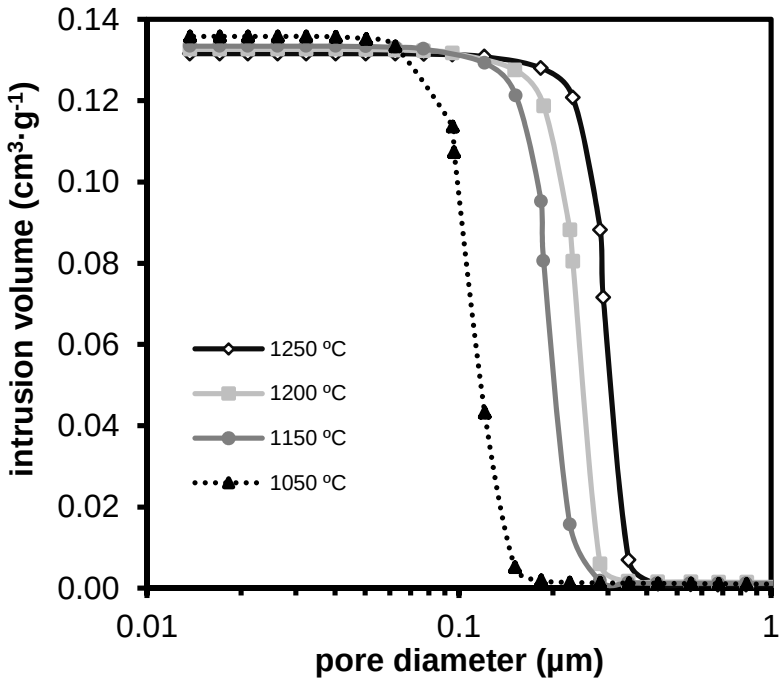

Figure 5. Pore size distribution of specimens sintered at different temperatures.

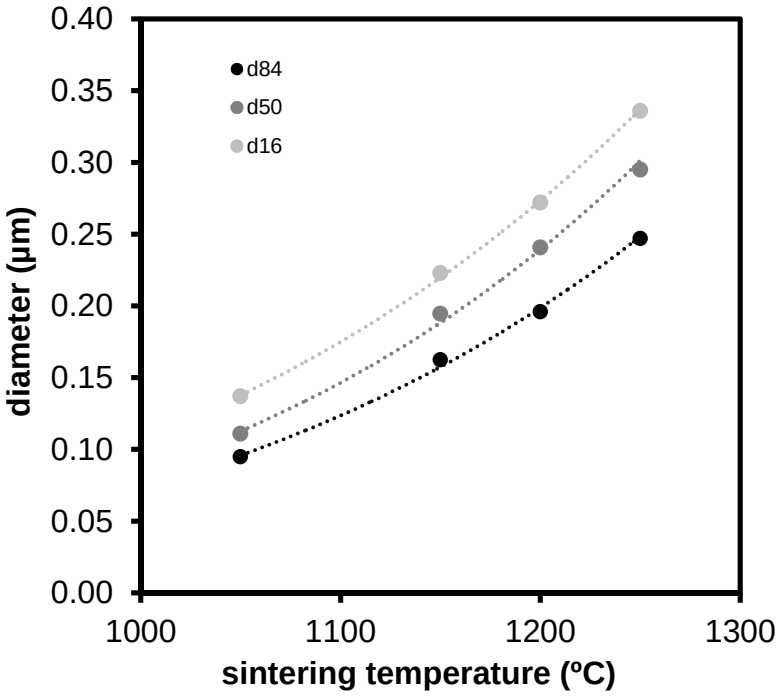

Figure 6. Evolution of mean pore diameters with sintering temperature.

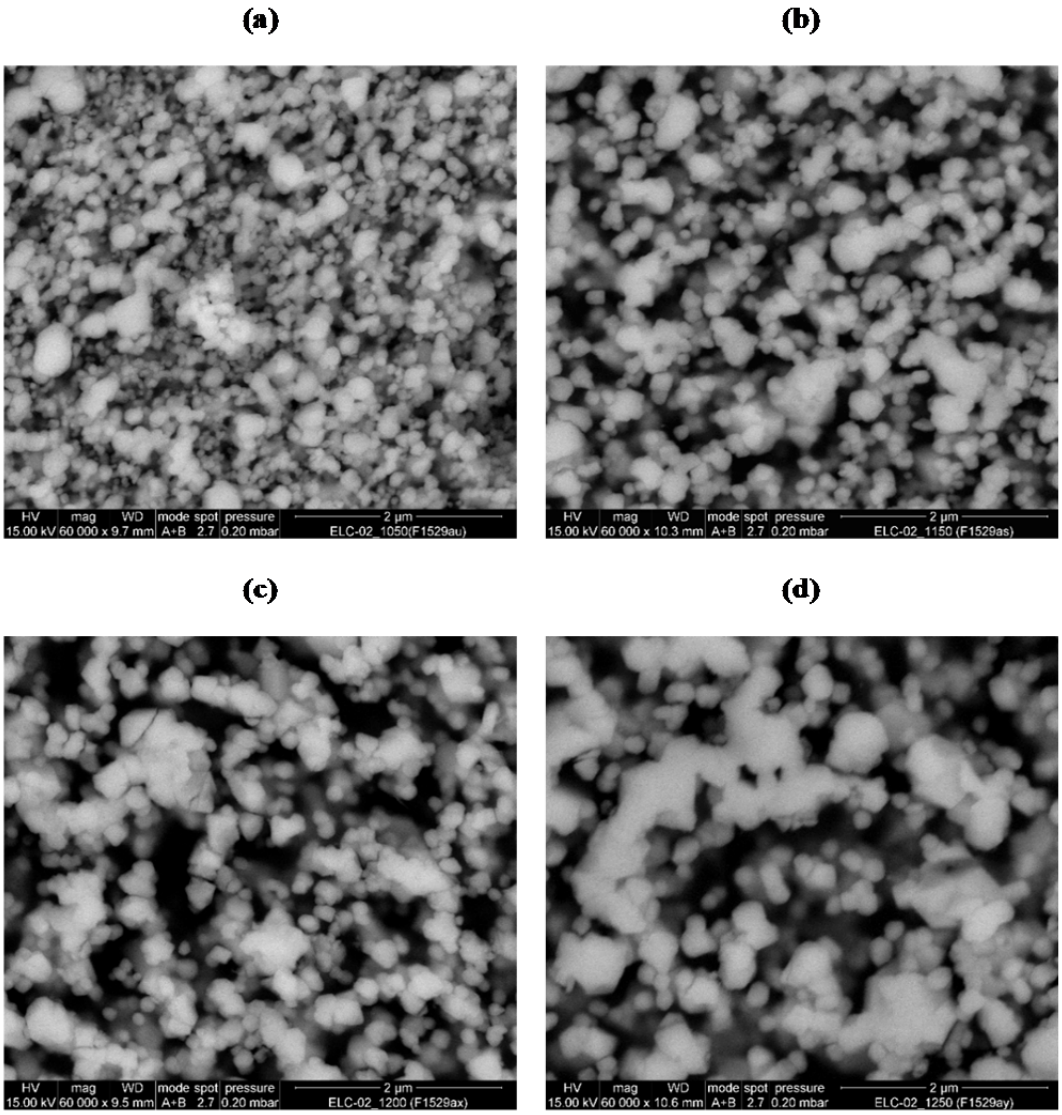

Figure 7. Evolution of specimen's microstructure with sintering temperature: (a) 1050 °C; (b) 1150 °C; (c) 1200 °C and (d) 1250 °C.

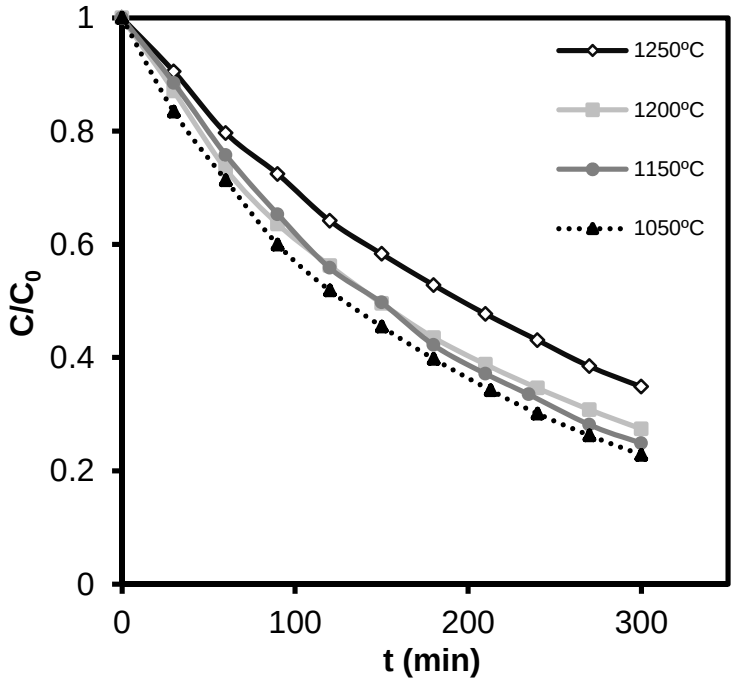

Figure 8. Degradation of Norfloxacin vs time for the ceramic electrodes as a function of the sintering temperature at an applied current of 15 mA.

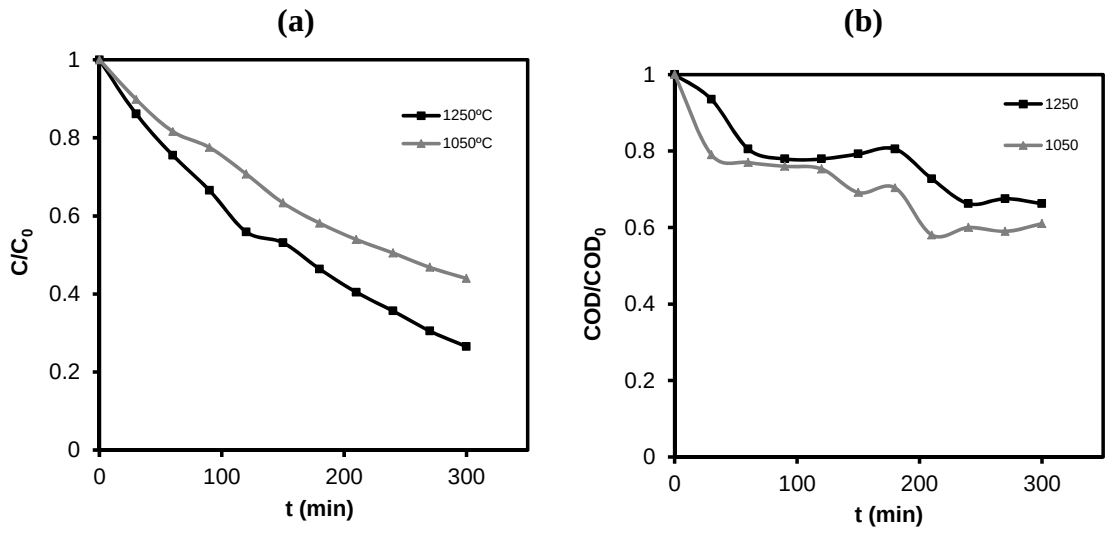

Figure 8. (a) Degradation of Norfloxacin and (b) COD removal vs time for two different ceramic electrodes (sintered at 1050 and 1250 ºC) at an applied potential of 2.5 V.

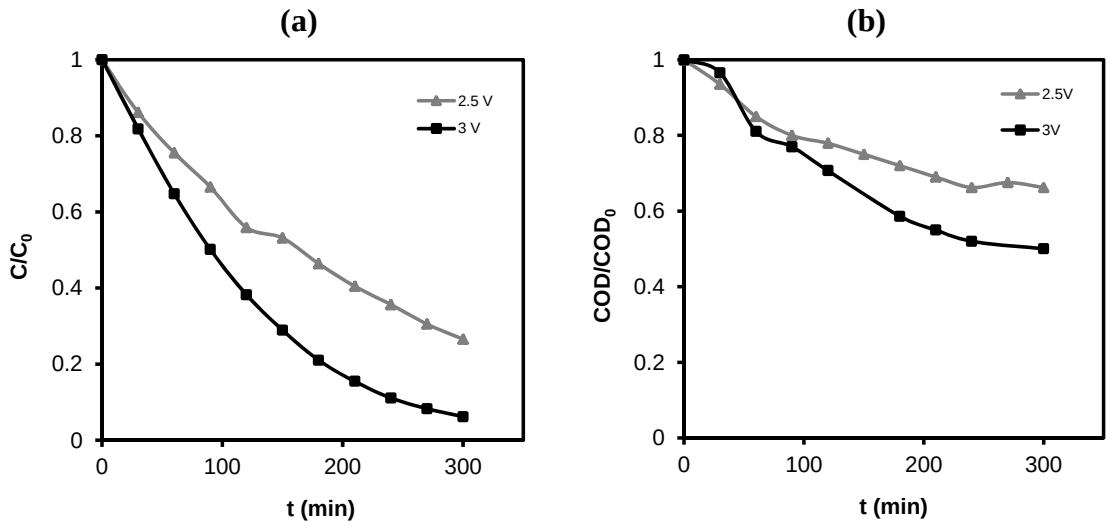

Figure 9. (a) Degradation of Norfloxacin and (b) COD removal vs time for the ceramic electrode sintered at 1250 ºC at an applied potential values of 2.5 and 3 V.

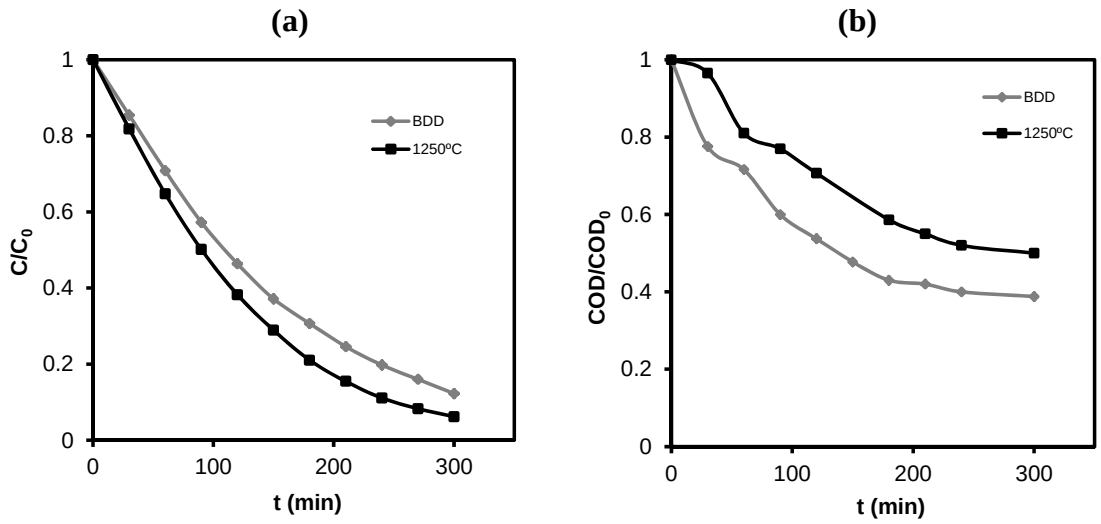

Figure 10. (a) Degradation of Norfloxacin and (b) COD removal vs time for the ceramic electrode sintered at 1250 ºC and for the BDD electrode at an applied potential of 3 V.

Table 2. Values of E_{O2} for each electrode in a 2 g/l Na_2SO_4 solution.

	1050 °C	**1150 °C**	**1200 °C**	**1250 °C**	**Pt**	**BDD**
E_{O2} (V)	2.033	1.911	1.889	1.873	1.561	2.500